Gruber, C., Abrykosov, O. (2016): On computation and use of Fourier coefficients for associated Legendre functions. - *Journal of Geodesy*, *90*, 6, pp. 525—535.

DOI: http://doi.org/10.1007/s00190-016-0891-z

On computation and use of Fourier coefficients for associated Legendre functions

Christian Gruber · **Oleh Abrykosov**

Received: date / Accepted: DOI: 10.1007/s00190-016-0891-z

Abstract The computation of spherical harmonic series in very high resolution is known to be delicate in terms of performance and numerical stability. A major problem is to keep results inside a numerical range of the used data type during calculations as under-/overflow arises. Extended data types are currently not desirable since the arithmetic complexity will grow exponentially with higher resolution levels. If the associated Legendre functions are computed in spectral domain then regular grid transformations can be applied highly efficiently and convenient for derived quantities as well. In this article we compare three recursive computations of the associated Legendre functions as trigonometric series, thereby ensuring a defined numerical range for each constituent wave-number, separately.

The results to high degree and order show the numerical strength of the proposed method. First, the evaluation of Fourier coefficients of the associated Legendre functions has been done with respect to the floating-point precision requirements. Secondly, the numerical accuracy in the cases of standard `Double` and `long Double` precision arithmetic is demonstrated. Following Bessel's inequality the obtained accuracy estimates of the Fourier coefficients are directly transferable to the associated Legendre functions themselves and to derived functionals as well. Therefore, they can provide an essential insight to modern geodetic applications that depend on efficient spherical harmonic analysis and synthesis beyond [5 × 5] arcmin resolution.

Keywords Associated Legendre Functions · Floating Point Accuracy · Fourier Coefficients · Spherical Harmonic Analysis · Spherical Harmonic Synthesis.

Ch. Gruber and O. Abrykosov
German Reserach Center for Geosciences, GFZ
Tel.: +49-8153-281586
Fax: +49-8153-281753
E-mail: gruber@gfz-potsdam.de

1 Introduction

The associated Legendre functions (hereinafter: Legendre functions) and their derivatives are of fundamental importance in various disciplines from classical to space geodesy, in geophysics, astronomy and nowadays even in biochemistry. Historically, they were calculated as closed power series (see e.g. Hobson 1955; Kaula 1966; Heiskanen and Moritz 1967). State of the art solutions are fast and precise computations by means of efficient recursive algorithms (see Holmes and Featherstone 2002; Claessens 2005; Jekeli et al. 2008). An external scaling to extend the numerical range of the functions has been proposed by Fukushima (2012).

Alternatively, and often overlooked, Legendre functions can be computed as finite trigonometric series, cf. Hofsommer and Potters (1960). Using this spectral approach for the computation of the basis functions has several advantages, such as direct access to derivatives of gravity functionals in each wave number k, respectively and high efficiency through fast Fourier expansions for the surface harmonics. This offers the possibility of fast spherical transformation of functions on the sphere (Gruber et al. 2011). For a comprehensive conceptual overview concerning surface spherical harmonics and Fourier methods, refer to Sneeuw and Bun (1996). Recursive relations for surface spherical harmonic expansions have already been described by Dilts (1985), and Elovitz et al. (1989) but not exceeding degree $l = 250$. Nowadays, with recent developments in high performance computer facilities, spherical harmonic coefficients can be aggregated and combined in a 2D FFT operator (Sneeuw and Bun 1996; Gruber et al. 2011; H. Cheong et al. 2012) to generate high resolution global data grid transformations with best possible performance. The computation of Fourier coefficients of Legendre functions by means of a convenient, simply applicable and numerically stable technique thus plays a fundamental role in such applications.

In this article, we focus on numerical studies of three techniques which are an immediate consequence of the second-order difference equations derived by Hofsommer and Potters (1960). These are: (i) forward recursion, (ii) backward recursion, (iii) Gaussian elimination and backward substitution.

In section 2, the necessary mathematical relationships are collected and derived. It is shown, that arbitrary non-zero starting values can be chosen for each of the considered techniques. The obtained coefficients can be easily re-normalized to actual values, afterward. The requirements to floating-point precision are investigated in section 3 for each of the aforementioned techniques whereas the numerical accuracy when using standard floating-point data types is evaluated in section 4. It is shown that backward recursion provides numerically most stable results and is well suitable for geodetic applications involving high resolution spherical harmonic analysis and synthesis using current standard numerical data types. Section 5 concludes the paper.

2 Fourier coefficients of the associated Legendre functions

Hofsommer and Potters (1960) have considered normalized associated Legendre functions of degree $l \geqslant 0$ and order $m \in [\,0,\, l\,]$, expressed in the form of finite sums

$$\overline{\overline{P}}_{lm} = \sum_{k=0\,(1)}^{l} a_{lmk} \begin{cases} \cos k\,\vartheta & (m-\text{even}) \\ \sin k\,\vartheta & (m-\text{odd})\,, \end{cases} \tag{1}$$

where summation is performed with stepsize 2 starting from 0 for even l and from 1 otherwise (thus l and k are always of same parity); $\vartheta \in [\,0,\, \pi\,]$ is the polar angle or co-latitude. The normalization, that holds equally for $m \in [\,-l,\, l\,]$, reads

$$\overline{\overline{P}}_{lm} = \sqrt{\frac{2l+1}{2} \cdot \frac{(l-m)!}{(l+m)!}}\, P_{lm}\,. \tag{2}$$

The simple relation with fully normalized Legendre functions $\overline{P}_{lm}$ reads

$$\overline{P}_{lm} = \sqrt{2(2-\delta_{0m})}\, \overline{\overline{P}}_{lm}\,, \tag{3}$$

where δ_{0m} is the usual Kronecker delta.

The Fourier coefficients a_{lmk} for each pair of degree l and wave number $k \leqslant l$ are connected by the second order difference equation (Hofsommer and Potter 1960) with respect to m:

$$\begin{aligned}(-1)^m\ &\gamma_{lm}\, a_{l,m-1,k} + 2k\, a_{lmk} + \\ &(-1)^{m+1} \gamma_{l,m+1}\, a_{l,m+1,k} = 0,\end{aligned} \tag{4}$$

where

$$\gamma_{lm} = \sqrt{(l+m)(l-m+1)}\,. \tag{5}$$

Closed expressions for $m = 0$ and $k = 0$ (which appears only if l, m are even) have been derived (Hofsommer and Potters, 1960) in the form

$$a_{l0k} = (2-\delta_{0k})\sqrt{(2l+1)/2}\ \cdot p_{(l-k)/2}\ p_{(l+k)/2} \tag{6}$$

$$a_{lm0} = \sqrt{(2l+1)/2}\sqrt{p_{(l-m)/2}\ p_{(l+m)/2}}\ \cdot p_{l/2}\,, \qquad m = 0,2,4,\ldots\,. \tag{7}$$

The factors $p_j = 2^{-2j}\binom{2j}{j}$ satisfy the recursive relation

$$p_0 = 1; \quad p_j = (1 - \frac{1}{2j})\ p_{j-1}\,. \tag{8}$$

The above equations give a mathematical basis to compute all coefficients for $m \geqslant 0$. As Eq. (7) exists, we will assume $k > 0$ in all further derivations.

2.1 Forward recursion

For $m = 0$, Eq. (4) reads

$$\gamma_{l0}\, a_{l,-1,k} + 2k\, a_{l0k} - \gamma_{l1}\, a_{l1k} = 0\,. \tag{9}$$

Taking into acount that $\gamma_{l0} = \gamma_{l1}$ and invariance under a change in sign for m, $\overline{\overline{P}}_{l,-1} = -\overline{\overline{P}}_{l1}$ and therefore, $a_{l,-1,k} = -a_{l1k}$, we can rewrite Eq. (9) in the form

$$k\, a_{l0k} - \gamma_{l1}\, a_{l1k} = 0\,, \tag{10}$$

and write the forward recursion for a_{lmk} (with the help of Eq. 4):

$$\begin{aligned} a_{l1k} &= \frac{k}{\gamma_{l1}}\, a_{l0k}\,, \\ a_{l,m+1,k} &= (-1)^m\, \frac{2k}{\gamma_{l,m+1}}\, a_{lmk} \\ &\quad + \frac{\gamma_{l,m}}{\gamma_{l,m+1}}\, a_{l,m-1,k} \quad (1 \leqslant m < l)\,. \end{aligned} \tag{11}$$

2.2 Gaussian elimination and backward substitution

Hofsommer and Potters (1960) have further pointed out that a symmetric tri-diagonal system of linear equations can be composed for each valid pair (l, k) on the basis of Eq. (4), and then solved for the coefficients a_{lmk}.

For $k > 0$, Eq. (10) can be rewritten as

$$2k\, a_{l0k} - \gamma_{l1}\, a_{l1k} = k\, a_{l0k}\,. \tag{12}$$

For $m = l+1$, we have $\gamma_{l,l+1} = 0$ from Eq. (5). Indeed, all Legendre functions where the order exceeds the degree vanish identically (Hofsommer and Potters, 1960), resulting for $m = l$,

$$(-1)^l\ \gamma_{ll}\, a_{l,l-1,k} + 2k\, a_{llk} = 0\,. \tag{13}$$

Therefore, the system from Eq. (4) becomes

$$\begin{pmatrix} 2k & -\gamma_{l1} & & \cdots & 0 \\ -\gamma_{l1} & 2k & \gamma_{l2} & & \\ & \gamma_{l2} & 2k & -\gamma_{l3} & \vdots \\ \vdots & & & \ddots & \\ & & & & (-1)^l\gamma_{ll} \\ 0 & \ldots & & (-1)^l\gamma_{ll} & 2k \end{pmatrix} \begin{pmatrix} a_{l0k} \\ a_{l1k} \\ a_{l2k} \\ \vdots \\ a_{llk} \end{pmatrix} = \begin{pmatrix} k\,a_{l0k} \\ 0 \\ 0 \\ \vdots \\ 0 \end{pmatrix} .$$

Gaussian elimination at Eq. (12) first, and then consequently at Eq. (4) for $m = 1, 2, \ldots l-1$, and finally at Eq. (13) leads to the equivalent upper bi-diagonal system

$$\begin{aligned} \beta_{lmk}\, a_{lmk} + (-1)^{m+1}\gamma_{l,m+1}\, a_{l,m+1,k} &= \lambda_{lmk} \;\; (0 \leqslant m < l), \\ \beta_{llk}\, a_{llk} &= \lambda_{llk} \;\; (m = l). \end{aligned} \tag{14}$$

The elements β_{lmk} of the main diagonal and λ_{lmk} of the right-hand side of this system fulfill the recursions ($m > 0$):

$$\beta_{l0k} = 2k; \quad \beta_{lmk} = 2k - \gamma_{lm}^2/\beta_{l,m-1,k}\,, \tag{15}$$

$$\lambda_{l0k} = k\,a_{l0k};\; \lambda_{lmk} = (-1)^{m-1}\lambda_{l,m-1,k}\gamma_{lm}/\beta_{l,m-1,k}\,, \tag{16}$$

where symmetry has been used and a_{l0k} is provided by Eq. (6). The last equation from Eq. (14) provides a result for the coefficients of the sectorial Legendre functions $\overline{\overline{P}}_{ll}$:

$$a_{llk} = \lambda_{llk}/\beta_{llk}\,. \tag{17}$$

The solutions for $m < l$ can now be computed by backward substitution of a_{lmk} into Eq. (14):

$$a_{lmk} = \left(\lambda_{lmk} + (-1)^m\gamma_{l,m+1}\, a_{l,m+1,k}\right) / \beta_{lmk} \quad (l > m)\,. \tag{18}$$

2.3 Backward recursion

From Eq. (6) and Eq. (16) we can conclude

$$a_{llk} \neq 0 \quad \forall \quad k > 0\,. \tag{19}$$

Therefore, the backward recursion for a_{lmk} follows immediately from Eq. (13) and Eq. (4):

$$\begin{aligned} a_{l,l-1,k} &= (-1)^{l-1} 2k\, \gamma_{ll}^{-1}\, a_{llk}\,, \\ a_{l,m-1,k} &= (-1)^{m-1} 2k\, \gamma_{lm}^{-1}\, a_{lmk} \\ &\quad + \gamma_{l,m+1}\, \gamma_{lm}^{-1}\, a_{l,m+1,k} \quad (l > m \geqslant 1)\,. \end{aligned} \tag{20}$$

For this recursion starting values a_{llk} have to be known. On the basis of the binomial power series (Hobson 1955) for the sectorial Legendre functions, Gruber (2011) has derived these starting values and proposed the respective scaling to avoid underflow issues during the computation of a_{lmk}. Alternatively, we already have the starting values, Eq. (17), after the Gaussian elimination. Moreover, in the next section we will find, that a starting value can be arbitrarily chosen.

2.4 Generic forms of the recursions

Recalling Eqs. (11, 18 and 20) it can be concluded that any non-zero value can be chosen as initial value for each of the three considered recursions, resulting in a linear shift of the numerical range used for the computations. Taking the initial value $\tilde{a}_{l0k} = 1$, and applying either forward recursion or Gaussian elimination followed by backward substitution we get coefficients $\tilde{a}_{lmk}$ which then have to be re-normalized by the actual value for a_{l0k} from Eq. (6):

$$a_{lmk} = \tilde{a}_{lmk} \cdot a_{l0k} \quad (0 \leqslant m \leqslant l). \tag{21}$$

Similarly, taking the initial value $\tilde{a}_{llk} = 1$ and applying the backward recursion we get coefficients $\tilde{a}_{lmk}$ which then have to be re-normalized by the ratio of the final coefficient $\tilde{a}_{l0k}$ and its closed solution from Eq. (6):

$$a_{lmk} = \tilde{a}_{lmk} \cdot (a_{l0k} \,/\, \tilde{a}_{l0k}) \quad (0 \leqslant m \leqslant l). \tag{22}$$

Thereby, no actual starting value is required for any of the three methods. This gives us an excellent opportunity to analyze the numerical behavior of these recursions in a relative sense, i.e. independent of the starting values.

3 Requirements to floating-point precision

Using the generic form of the recursions, we have examined the necessary floating-point precision that preserves a predefined accuracy ε (i.e. number of accurate decimal digits) of Fourier coefficients a_{lmk}. Each recursion $r(b_i)$ has been computed with the length of mantissas fixed to b_i ($b_0 < b_1 < b_2 \ldots$) bits. Computations were then repeated until $|r(b_i) \;/r(b_{i+1}) - 1| < \varepsilon$, and the value b_i was considered as the requested floating-point precision. This algorithm has been implemented using the multiple-precision binary floating-point library MPFR (`http://www.mpfr.org`) because it allows to fix mantissa lengths with a step of 1 bit and keep mantissa and exponent separately, thus making computations free of numerical under-/overflow issues.

Each of the three techniques has been applied in generic form for $l = k = 10800$. Table 1 illustrates examples of these estimations prepared with $\varepsilon = 10^{-18}$. It is seen how convergence is reached to guarantee mantissas to be accurate to 18 decimal digits. It becomes clear that forward recursion is highly demanding concerning digital number representation in order to preserve accuracy. Note that backward recursion is computed in inverse direction to forward recursion and Gaussian elimination, both starting from generic $a_{l0k} = 1.0$. Therefore, they correspond to each other inversely, compare Eq. (22).

For the relevancy of numerical coefficient precision, refer also to Appendix B that provides the mean square errors for the Legendre Functions.

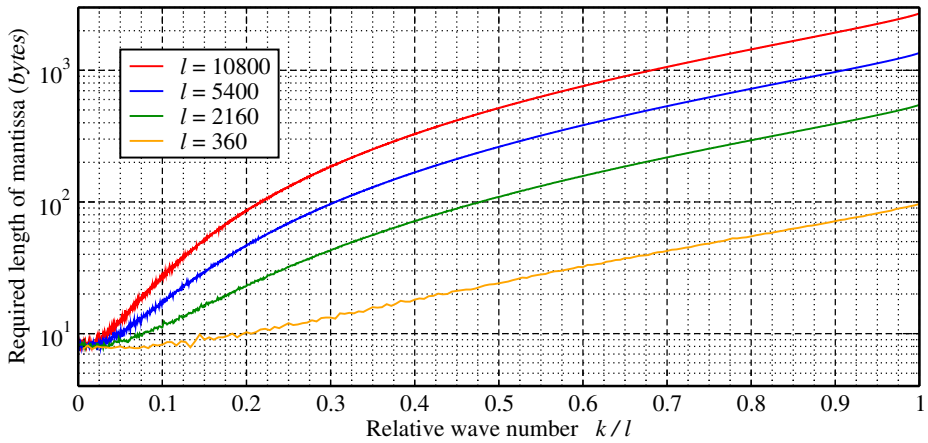

Fig. 1 Forward recursion: floating-point precision that is necessary to compute $\tilde{a}_{llk}$ accurate to 18 decimal digits. With double precision numbers only zero and near zero wave numbers can be computed stable. For the higher frequencies the number of required digits grows exponentially.

Table 1 Floating-point precision to perform computations. For each approach the result from the starting number of bits (53) and the required number to eventually set all mantissa digits to the proper value are displayed.

Required bits	Mantissa to 18 decimal digits	Decimal exponent
	Forward recursion	
53	−2.19 02699 83653 55848	+3234
21653	+1.02 02174 54251 11277	−3250
	Gaussian elimination	
53	+1.02 02174 54251 02563	−3250
65	+1.02 02174 54251 11277	−3250
	Backward recursion	
53	+9.80 18319 11746 78844	+3249
69	+9.80 18319 11747 15465	+3249

Fig. 1 displays the results of the evaluation of the forward recursion, Eq. (11). Again, $\varepsilon = 10^{-18}$ was used to guarantee mantissas to be accurate to 18 decimal digits and the very last result (the coefficients $\tilde{a}_{llk}$) of the recursion has been checked at each wave number k. One can see that computations with short mantissas (corresponding to standard `Double` or even `Quadruple` precision) can provide accurate results only for very small wave numbers k, whereas for higher wave-numbers the requirements to mantissa length will grow exponentially. An explanation for this behavior can be given if we take into account that γ_{lm} decreases monotonically with increasing m:

$$\frac{\mathrm{d}\gamma_{lm}}{\mathrm{d}m} = \frac{1-2m}{2\gamma_{lm}} < 0\,, \quad \forall\, m > 0\,. \tag{23}$$

Then, both ratios, $2k/\gamma_{l,m+1}$ and $\gamma_{lm}/\gamma_{l,m+1}$ grow monotonically in Eq. (11) and the latter ratio is always greater than 1, while the coefficients a_{lmk} are decreasing. Therefore, a strong amplification of accumulated round-off errors can be expected since different signs for both ratios lead to annihilation of digits during subtraction. During the backward recursion this, on the opposite, is suppressed. The amplification leads to the necessity to operate with extremely long mantissas that makes the forward recursion practically not applicable. Note that this numerical 'instability' was already pointed out by Hofsommer and Potters (1960).

3.1 Deficient results with Gaussian Elimination

Unlike the forward recursion, the solutions based on Gaussian elimination followed by backward substitution as well as the solutions based on backward recursion can deliver high accuracy of the results using reasonable short ($60-70$ bits) mantissas for all wave-numbers k. Figure 2 displays the assessment of floating-point precision requirements for these two techniques. Here the very last results (the coefficients $\tilde{a}_{l0k}$) have been examined against $\varepsilon = 10^{-18}$.

However, when comparing more closely the results from the Gaussian elimination with those from the backward recursion, one can see (cf. top and bottom plots in Fig. 2) that the former technique requires a higher floating-point precision for small wave numbers k. The appearance of small diagonal elements β_{lmk} in the equivalent upper bi-diagonal system, Eq. (14), can be pointed out as a cause for this requirement.

To illustrate the impact of small diagonal elements we have computed β_{lmk} from Eq. (15) for $1 \leqslant l \leqslant 10800$, with all valid wave numbers $0 < k \leqslant l$. The smallest absolute value $|\beta_{lmk}| = 2\cdot 10^{-8}$ was found for $l = 6135, k = 4513, m = 2461$. Then, the floating-point precision required by the Gaussian elimination to compute all coefficients $\tilde{a}_{l=6135,m,k=4513}$ has been evaluated against $\varepsilon = 10^{-18}$. The results, see top plot in Fig. 3, demonstrate an impressive jump (close to 32 bits) of precision requirements for all coefficients of orders $m \leqslant 2461$ when computed from Eq. (18). This jump disap-

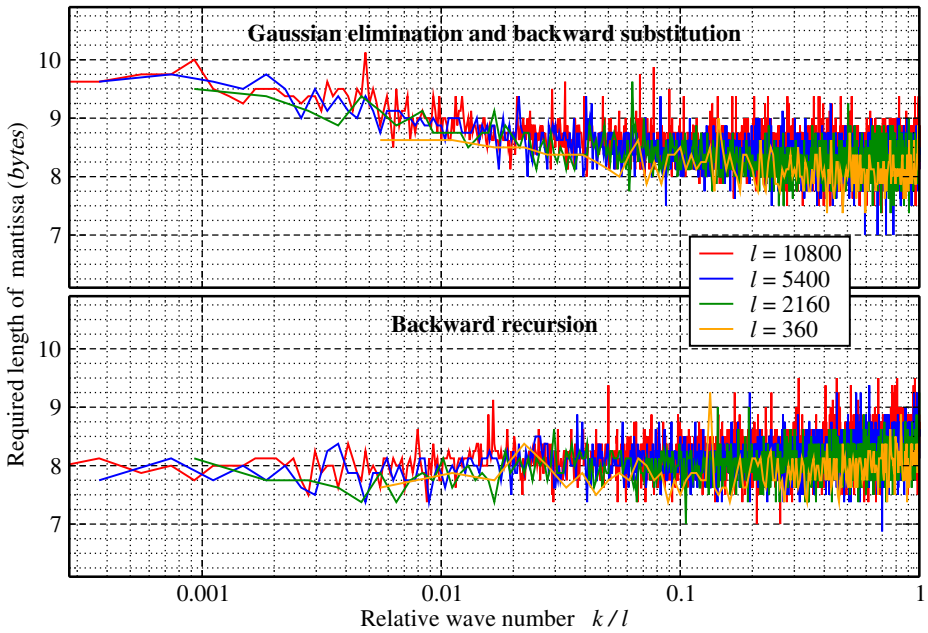

Fig. 2 Gaussian elimination and backward substitution against backward recursion: floating-point precisions that are necessary to compute a_{l0k} accurate to 18 decimal digits.

peared completely if the backward recursion is applied instead of the Gaussian elimination followed by the backward substitution and explains why a higher floating-point precision for the small wave numbers is required in Fig. 2.

For the sake of consistency, the same evaluation of the two discussed techniques has been done for the next wave number $k = 4515$ of the same degree $l = 6135$. The smallest diagonal element $|\beta_{lmk}| = 7$ was found in this case at $m = 2341$. A very homogeneous requirement to floating-point precision for both techniques is found (bottom plot in Fig. 3).

Thus, the numerical accuracy of results obtained from the Gaussian elimination and backward substitution can be degraded to a large extent when small divisors appear. In this view, the backward recursion seems to be the preferable numerical approach to compute Fourier coefficients of associated Legendre functions.

4 Results for fixed length mantissas

From Tab. 1 we have selected Gaussian elimination or backward recursion as prospective methods for further studies with standard precision floating-point representations (`Double`, `long Double`, `Quadruple`). However, with these standard representations (Tab. 2) an underflow occurs for high degrees l and high wave numbers k during Gaussian elimination whereas an overflow occurs during backward recursion (Tab. 1, third column). To overcome these problems, a dynamical scaling (modification of exponents by using `frexp` and `ldexp` functions from the standard C library) has been applied. It is important to note, that the scaling has no impact on the computed mantissas. For a comprehensive description of the principles of exponent extension, the reader is referred to Fukushima (2012).

Table 2 Floating point numbers according to IEEE standard.

Name	`Double`	`long Double`	`Quad`
mantissa length	53	64	113
binary exponent	±1021	±16381	±16381
precision(decimal)	15	18	33
decimal exponent	±307	±4931	±4931
machine epsilon	2.2e−16	1.1e−19	1.9e−34

The relative accuracies obtained with `Double`, `long Double` and `Quadruple` precision are obtained by comparing the final a_{l0k} from Eqs. (18, 20) against the closed form in Eq. (6) and are shown in Fig. 4. It is again revealed that a significant loss of accuracy throughout the wave-numbers occurs, when Gaussian elimination with backward substitution is used (blue lines). Note, that this happens no matter how many digits are used for the mantissa. Application of backward recursion after Gaussian elimination instead of substitution in a 'mixed solution', starting from Eq. (17) mitigates this problem to a large extent (green lines) but still leaves some (low) wave-numbers significantly less accurate than the direct application of backward recursion in the generic form (red lines). Here, the relative error linearly increases with increasing wave-numbers but preserves at least one or-

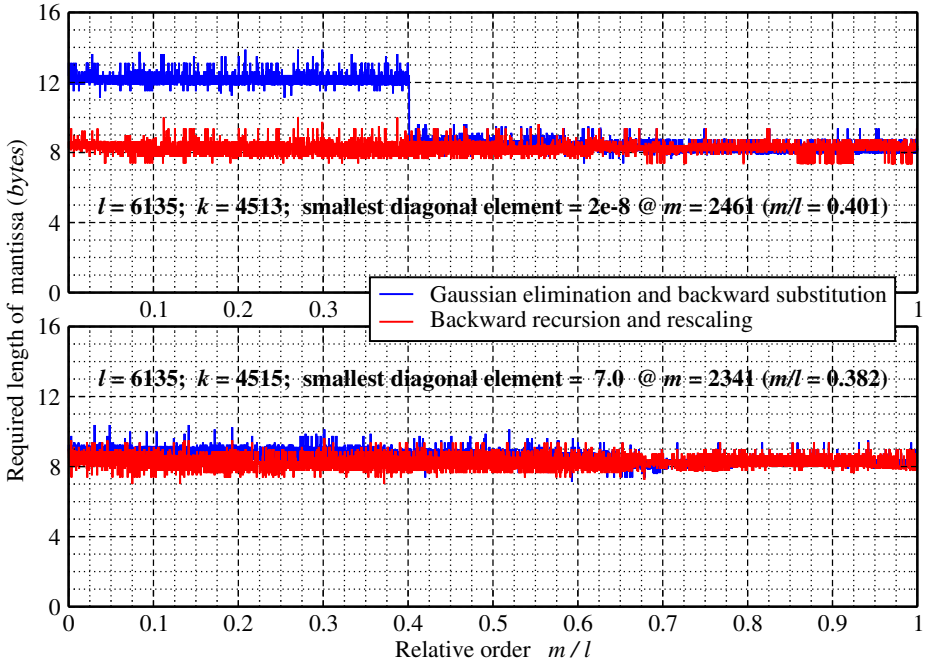

Fig. 3 Impact of small diagonal elements on the floating-point precision required by the Gaussian elimination and backward substitution.

der of magnitude higher accuracy than compared to the Gaussian elimination. This strength in especially the lower frequencies of the Legendre functions, we believe, makes this numerical approach the method of choice for high resolution computations in the aforementioned standard numerical representations.

Next, we have made use of the following formulae (Hofsommer and Potters, 1960) to check all resulting coefficients, belonging to a respective order

$$\sum_{k=0}^{l} a_{2l,2m,2k} = \sqrt{2l+\tfrac{1}{2}}\,\delta_{m0}\,, \tag{24}$$

$$\sum_{k=1}^{l} a_{2l,2m+1,2k} = \frac{p_l}{2m+1}\sqrt{(2l+\tfrac{1}{2})} \times \sqrt{(2l-2m-1)\,p_{l+m}\cdot p_{l-m-1}}, \tag{25}$$

$$\sum_{k=0}^{l} a_{2l+1,2m,2k+1} = \sqrt{2l+1\tfrac{1}{2}}\,\delta_{m0}\,, \tag{26}$$

$$\sum_{k=0}^{l} (-1)^k a_{2l+1,2m+1,2k+1} = (-1)^{l-m} \times \sqrt{(2l+1\tfrac{1}{2})\,p_{l+m+1}\cdot p_{l-m}}\,. \tag{27}$$

We have computed misclosures of these relations for all Legendre functions of degrees from 1 to 21600 using the backward recursion for the Fourier coefficients and two different standard levels of floating-point precision: `Double` precision (53-bit mantissas) and `long Double` precision (64-bit mantissas). The results (Fig. 5), demonstrate that in both cases the accumulated misclosures remains in good agreement with the relative error corresponding to the fixed length of the mantissas. Even in double precision the misclosure is $\sim 10^{-14}$ at degree $l = 10800$ (better than 2 km resolution) and does not exceed 10^{-13} at degree $l = 21600$ (better than 1 km resolution).

A similar test has been initially found (for inclination functions) by Wagner (1983) providing the degree-wise errors for the Fourier coefficients. We consider this test as the degree deficit (d_l^2) of the basis functions, adopted to the coefficients of the Legendre functions

$$d_l^2 = \left| (2l+1) - \sum_{m=0}^{l} (2-\delta_{m0}) \sum_{k=0(1)}^{l} (2-\delta_{k0})\, a_{lmk}^2 \right|\,, \tag{28}$$

as an indicator of stability during the recursions. Comparison of these values for backward recursion and Gaussian elimination followed by backward substitution in Fig. 6 reveals that there is a systematic degradation for the latter approach by approximately two orders of magnitude with huge peaks caused by the impact of small diagonal elements, as already been discussed in section 3. Therefore, the backward recursion can be recommended as the method of choice when computing Fourier coefficients of associated Legendre functions, e.g. for the high resolution spherical harmonic modeling of the Earth's gravity field.

Based on this finding, we estimate the impact of the degree deficits for the backward recursion by using Kaula's rule of thumb ($10^{-5} \times l^{-2}$) on three different gravity signals,

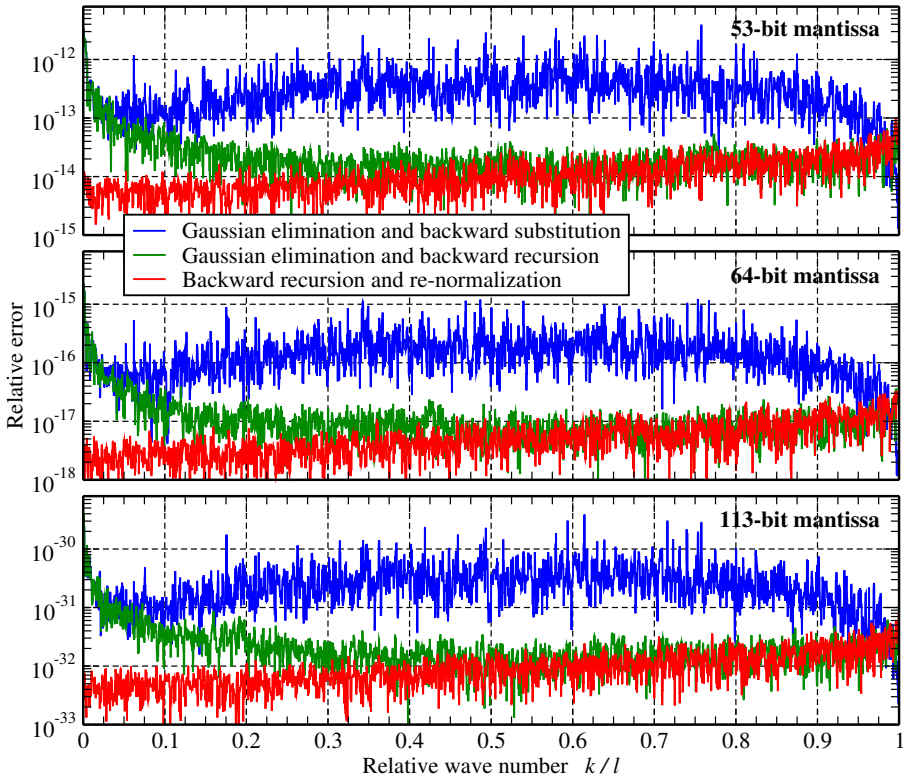

Fig. 4 Relative accuracy of a_{l0k} computed for $l = 10800$ with backward recursion after re-normalization with Eq. (22) compared to Gaussian elimination with different backward solutions.

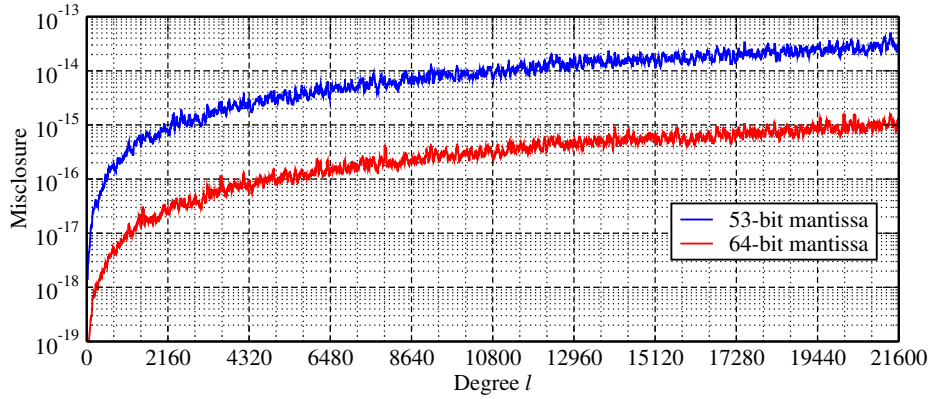

Fig. 5 Total misclosure from the invariants for all orders and frequencies to each degree l according to Eqs. (24–27), computed by backward recursion.

geoid height, gravity disturbance and radial gravity gradient,

$$\sigma_l(N) = R \cdot l^{-2} d_l \times 10^{-2} \quad [\text{mm}] \tag{29}$$

$$\sigma_l(\delta g) = \frac{GM}{R^2}(l+1)\, l^{-2} d_l \quad [\text{mGal}] \tag{30}$$

$$\sigma_l(V_{rr}) = \frac{GM}{R^3}(l+2)(l+1)\, l^{-2} d_l \times 10^4 \quad [\text{E}]\,. \tag{31}$$

where GM is Earth gravitational constant and R is the radius of the reference sphere (6378137 m), N is geoid height in [mm] (10^{-3} m), δg is gravity disturbance given in [mGal] (10^{-5} ms^{-2}) and V_{rr} is the radial derivative of gravity in [Eötvös] (10^{-9} s^{-2}). The results in Fig. 7, computed in standard `Double` precision clearly show, that the projected errors for all three signals remain below physical significance. Also, it should be noted that these projected errors are rather too pessimistic, because the rule is known to overestimate the spectral power of the Earth's gravity field for high degrees.

For a theoretical discussion on the propagation of round-off errors in the coefficients into the functional domain, see the appendix B.

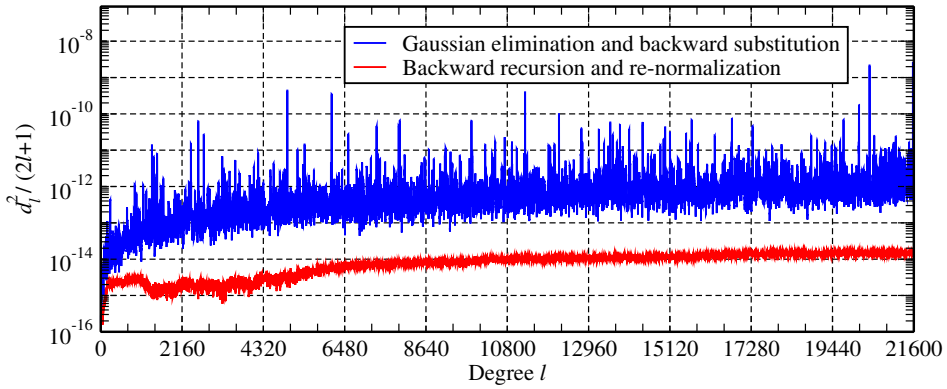

Fig. 6 Degree deficits according to Eq. (28) computed with double precision.

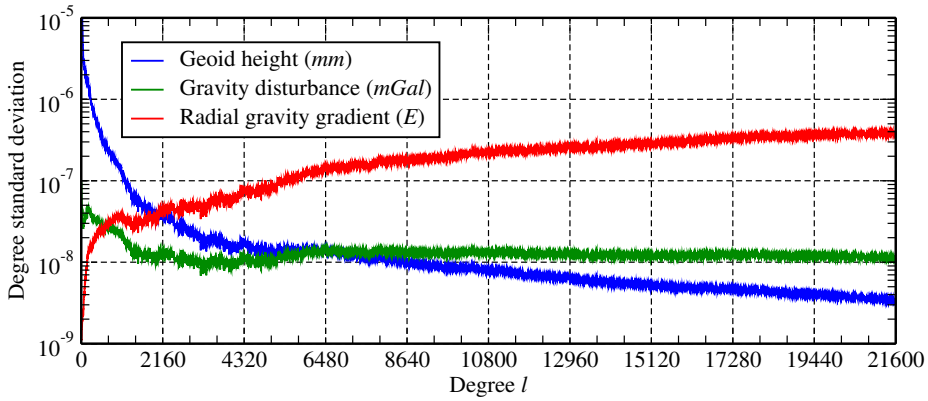

Fig. 7 Estimated degree standard deviation per degree l according to Eqs. (29–31), computed by backward recursion. Note, that these estimates are rather pessimistic because of too much spectral power in high degrees from the underlying Kaula's rule.

4.1 Global gravity field computation

To conclude the evaluation concerning the numerical precision and the computational performance a direct comparison of results from global spherical harmonic synthesis of an exemplary global gravity field with a spectral resolution of $l_{max} = 5400$, has been applied. The global gravity field was created based on EGM2008 and additional influences from residual terrain. The gravity anomaly on the sphere is defined as

$$\Delta g = \frac{\mathrm{GM}}{R^2} \sum_{l=0}^{l_{max}} (l-1) \sum_{m=0}^{l} \bar{P}_{lm}(\cos\theta)\,(\bar{C}_{lm}\cos m\lambda + \bar{S}_{lm}\sin m\lambda) \tag{32}$$

where $\bar{C}_{nm}, \bar{S}_{nm}$ are normalized coefficients of the spherical harmonic expansion.

We have computed a synthesis via backward recursion consistent in the Fourier domain (FFT) according to Gruber et al. (2011) using the spectral coefficients subject to this paper. Then once again by following a standard (degree-wise) synthesis with dynamic exponent scaling using the generic functions `frexp` and `ldexp` from the standard C-libraries during the computation of the Legendre functions. In order to have a trustworthy reference we repeated the latter for the `long Double` data type as well. We then compared these three solutions to a forth solution, that was obtained from 'GSHS' (Sneeuw, 1994) using 1D fast Fourier transformation for the longitude expansion and recursively computed Legendre functions (cf. Koop and Stelpstra 1989) that we adopted to dynamical scaling, as well. Here we used an individual solution to the problem based on external scaling numbers that are invoked in the case of under-/overflow appearance, see appendix B for further details.

To give a hint on the relative computation times (in single thread execution) we achieved 24 minutes using the Fourier approach, 114 minutes with our dynamically scaled standard synthesis (both as binary executables) and 189 minutes for the stabilized S-GSHS (matlab TM-script). The resulting global RMS differences in gravity anomalies (Gal) for each $[2' \times 2']$ arcmin data grid are listed in Tab. 3. The numerical error for each method is then shown in the first column as the synthesis with `long Double` can be considered as error free. The reference solution fits best with the full FFT approach (bold face). This confirms our effort to provide consistent Fourier coefficients for Legendre functions that can be used for ultra high resolution purposes.

Table 3 Global RMS differences in gravity anomalies [Gal]. DS abbreviates dynamic exponent stabilization and is a scaled standard synthesis using the standard C-libraries in `Double` and `long Double` (64-bit mantissa). FFT denotes backward recursion in Fourier domain (Eq. 20) and subsequent 2D-transform. The bold faced value indicates that this solutions fits best the reference solution. S-GSHS is the manually scaled GSHS. See also text for further explanations.

Legendre funcs	DS (64-bit)	DS	S-GSHS
DS	2.53e-17	0	
S-GSHS	1.69e-17	2.99e-17	0
FFT	**0.48e-17**	2.58e-17	1.76e-17

5 Conclusions

In order to compute Fourier coefficients of the associated Legendre functions three solutions, offering a frequency-wise processing and scaling have been investigated numerically.

The need for huge mantissas to preserve a predefined relative accuracy during the forward recursion has been confirmed. The increasing amount of necessary digits can be consigned to arbitrary precision libraries but truly at the cost of operational efficiency for the carried on computations. This makes the forward recursion not applicable in ultra-high resolutions.

With Gaussian elimination and the backward substitution no scaling factors have to be considered in practice, if threshold values are introduced during the elimination and the process is broken as it asymptotically approaches an underflow limit. Certainly, the elimination has turned out to be undependable, as for certain constellations (l,m,k) sudden loss in precision occurs probably due to the appearance of small divisors.

Initial values for the backward recursion can be chosen by convention (e.g. 1.0) and need not to be computed. This generic approach yields best performance in terms of computational efficiency as well as numerical stability throughout all wave-numbers belonging to a fixed spherical harmonic degree. The backward recursion shows no significant increase in mantissa requirements even for $5-$digit harmonic degrees.

Therefore, we conclude that the described backward recursion is practically most suited for the computations of Fourier coefficients of associated Legendre functions for the purpose of high resolution modeling of the Earth gravity field.

The Fourier coefficients give the opportunity to directly compute associated Legendre functions without recursions if they are precomputed and stored. For certain applications with repeated demand for specific functions, (e.g. $m = 0$) this can be advantageous.

The accuracy-level of global spherical harmonic transformations can be auto-controlled by invariants, that directly reveal the accuracy of the transformation.

Acknowledgements The authors have obtained valuable hints from Prof. Nico Sneeuw, Universität Stuttgart that have helped to improve the manuscript substantially. The software comparison was conducted with minor modifications concerning under-/overflow to software written by Nico Sneeuw at IAPG, TU-Munich 1994.

References

1. Cheong, H.B., Park, J.R., Kang, H.G.: Fourier-series representation and projection of spherical harmonic functions. Journal of Geodesy, Springer-Verlag. **86**, 975–990 (2012)
2. Claessens, S.J.: New relations among associated legendre functions and spherical harmonics. Journal of Geodesy **79**, 398–406 (2005)
3. Dilts, G.: Computation of Spherical Harmonic Expansion Coefficients via FFT's. Journal of Computational Physics **57**, 439–453 (1985)
4. Elovitz, M.: A Test of a Modified Algorithm for Computing Spherical Harmonic Coefficients Using an FFT. Journal of Computational Physics **80**, 506–511 (1989)
5. Fukushima, T.: Numerical computation of spherical harmonics of arbitrary degree and order by extending exponent of floating point numbers. Journal of Geodesy **86**, 271–285 (2012)
6. Gruber, C.: A study on the Fourier composition of the associated Legendre functions; suitable for applications in ultra-high resolution, (Scientific Techncial Report STR; 11/04). Deutsches GeoForschungsZentrum (GFZ) (2011)
7. Gruber, C., Novák, P., Sebera, J.: FFT-based high-performance spherical harmonic transformation. Studia Geophysica et Geodaetica **55**, 489–500 (2011)
8. Heiskanen, W.A., Moritz, H.: Physical & Geodesy. W.H. Freeman Company, San Francisco (1967)
9. Hobson, E.W.: The Theory of Spherical and Ellipsoidal harmonics. Chelsea Publishing Company, New York (1955)
10. Hofsommer, D.J., Potters, M.L.: Table of Fourier Coefficients of Associated Legendre Functions, Report R 478. KNAW, Computational Department of the Mathematical Centre, Amsterdam (1960)
11. Holmes, S.A., Featherstone, W.E.: A unified approach to the clenshaw summation and the recursive computation of very high degree and order normalised associated legendre functions. Journal of Geodesy **76**, 279–299 (2002)
12. Jekeli, C., Lee, J.K., Kwon, J.H.: On the computation and approximation of ultra-high-degree spherical harmonic series. Journal of Geodesy, Springer Verlag. **81**, 603–615 (2008)
13. Kaula, W.M.: Theory of Satellite Geodesy. Blaisdell Pub. Co., Waltham, Massachusetts (1966)
14. Koop, R. and Stelpstra D., 1989, On the computation of the gravitational potential and its first and second order derivatives, Manuscripta Geodaetica, Springer Verlag, Vol. 14, pages 373-382.
15. Sneeuw, N., Bun, R.: Global spherical harmonic computation by two-dimensional fourier methods. Journal of Geodesy **70**, 224–232 (1996)
16. Sansone, G.: Orthogonal Functions (1991). Reprint: Dover Publications, Inc., 31 East 2nd Street, Mineola, NY11501. Orig. published: Interscience, 1959. (Pure and applied mathematics: vol. 9)
17. Wagner, C.A.: Direct Determination of Gravitational Harmonics From Low-Low GRAVSAT Data. Journal of Geophysical Research **88**, 309–321, No. B12 (1983)

Appendix A

In order to demonstrate how the Fourier coefficient round-off errors will infiltrate the functional domain, we consider Bessel's inequality. Following Sansone (1991), we can use the theorem:

"Let $\{f_k\}$ be a sequence of orthonormal functions in σ, F square integrable in σ and $\{a_k\}$ is the sequence of Fourier coefficients with respect to $\{f_k\}$,

$$a_k = \int_\sigma F f_k \, d\sigma, \quad (k = 1,2,\ldots) \tag{33}$$

then the series

$$\sum_{k=0}^{\infty} a_k^2 \tag{34}$$

is convergent, and, moreover, the a_k will satisfy Bessel's inequality:

$$\sum_{k=0}^{\infty} a_k^2 \leqq \int_\sigma F^2 \, d\sigma. " \tag{35}$$

Concerning the round-off errors ε of our coefficients we put:

$$b_k = a_k + \varepsilon_k, \tag{36}$$

and for the square residuals of the finite series

$$\phi = \int_\sigma \left[P_{lm} - \sum_{k=0}^{N} b_k \, f_k \right]^2 d\sigma \, . \tag{37}$$

Note that $\sigma \in [0;2\pi]$ although the Legendre functions P_{lm} are known to be square integrable (i.e. they form another orthonormal system) only in $[0;\pi]$. However, we need only a well defined subset of the sequence of orthonormal functions $f_k' \subset f_k$, where the Fourier integrals may be used to obtain the appropriate coefficients a_{lmk}. These are (Eq. 1):

$$f_k' = \begin{cases} \cos k\,\vartheta & (m-\text{even}, \; l,k-\text{ even}), \\ \sin k\,\vartheta & (m-\text{odd}, \; l,k-\text{ even}), \\ \cos k\,\vartheta & (m-\text{even}, \; l,k-\text{ odd}), \\ \sin k\,\vartheta & (m-\text{odd}, \; l,k-\text{ odd}) \, . \end{cases} \tag{38}$$

In all other cases, $\int_0^{2\pi} P_{lm} \; f_k \; d\sigma$ are not guaranteed to be solved correctly. We then continue for the subset f_k' and obtain

$$\begin{aligned} \phi &= \int_\sigma P_{lm}^2 \, d\sigma + \sum_{k=0}^{N} b_k^2 \int_\sigma f_k'^2 + \\ &\qquad 2 \sum_{k \neq n} b_k \, b_n \int_\sigma f_k' \, f_n' \, d\sigma - 2 \sum_{k=0}^{N} b_k \int_\sigma P_{lm} \, f_k' \, d\sigma \\ &= \int_\sigma P_{lm}^2 \, d\sigma + \sum_{k=0}^{N} b_k^2 - 2 \sum_{k=0}^{N} b_k \, a_k \\ &= \int_\sigma P_{lm}^2 \, d\sigma + \sum_{k=0}^{N} (a_k^2 + 2a_k \, \varepsilon_k + \varepsilon_k^2) - 2 \sum_{k=0}^{N} (a_k^2 + a_k \, \varepsilon_k) \\ &= \int_\sigma P_{lm}^2 \, d\sigma - \sum_{k=0}^{N} a_k^2 + \sum_{k=0}^{N} \varepsilon_k^2 , \end{aligned} \tag{39}$$

where

$$\int_\sigma f_k f_n \, d\sigma = 0, \quad k \neq n; \quad \int_\sigma f_k^2 \, d\sigma = 1 \, . \tag{40}$$

Because the error-free solution is defined by

$$\int_\sigma \left[P_{lm} - \sum_{k=0}^{N} a_k \, f_k' \right]^2 d\sigma \equiv 0 \, , \tag{41}$$

we obtain for the square residuals

$$\phi = \sum_{k=0}^{N} \varepsilon_k^2 \, , \tag{42}$$

which corresponds to what we have been investigating throughout Eqs. (24–27) but also in Eq. (28) and can thus be considered as corresponding deviation in the functional domain.

Appendix B

The dynamical scaling works as follows: the sectorial Legendre Function ($l = m$) serves as starting value and is subject to numerical underflow such that extended exponent values have to be stored. In the course of the recursive computations of the respective degrees the external exponents are then partially re-applied before overflow values occur until the scales have fully dissolved.

%$\mathrm{S_c}$ vector of external scales with dimension : θ

% p vector of Legendre Functions

```
    p       = init                      %factorials
for i       = 1 : m
    p       = p · sin θ
    ip      = find(log|p| < −700)       %underflow?
    if      not empty(ip)
      s_c   = round(log|p(ip)|)         %extract exponent
      p(ip) = p(ip) · 2^(−s_c)          %and apply scaling
      S_c(ip) = S_c(ip) + s_c           %update scale
    end if
end
```

During l-recursion the Legendre functions are then re-scaled in the following way:

```
for  l        = m + 1 : lmax
     p        = func(p_−1, p_−2)        %l − recursion
     p_−2     = p_−1
     p_−1     = p
     ip       = find(log|p| > 700)      %overflow?
     if       not empty(ip)
       s_c    = max(−700, S_c(ip))      %partial scale
       p_−1(ip) = p_−1(ip) · 2^(s_c)    %dissolve scaling
       p_−2(ip) = p_−2(ip) · 2^(s_c)
       S_c(ip)  = S_c(ip) − s_c         %update scale
     end if
     p        = p_−1 · 2^(S_c)          %final re − scale
endif
```